

# Predicting distributional profiles of physical activity in the NHANES database using a Partially Linear Single-Index Fréchet Regression model

Aritra Ghosal<sup>\*2</sup>, Marcos Matabuena<sup>†1</sup>, Wendy Meiring<sup>§2</sup> and Alexander Petersen<sup>¶3</sup>

<sup>1</sup>CiTIUS (Centro Singular de Investigación en Tecnoloxías Intelixentes), Universidad de Santiago de Compostela.

<sup>2</sup>Department Statistics and Applied Probability, University of California, Santa Barbara.

<sup>3</sup>Department of Statistics, Brigham Young University.

February 16, 2023

## Abstract

Object-oriented data analysis is a fascinating and developing field in modern statistical science with the potential to make significant and valuable contributions to biomedical applications. This statistical framework allows for the formalization of new methods to analyze complex data objects that capture more information than traditional clinical biomarkers. The paper applies the object-oriented framework to analyzing and predicting physical activity as measured by accelerometers. As opposed to traditional summary metrics, we utilize a recently proposed representation of physical activity data as a distributional object, providing a more sophisticated and complete profile of individual energetic expenditure in all ranges of monitoring intensity. For this purpose of predicting these distributional objects, we propose a novel hybrid Fréchet regression model and apply it to US population accelerometer data from NHANES 2011–2014. The semi-parametric character of the new model allows us to introduce non-linear effects for essential variables, such as age, that are known from a biological point of view to have nuanced effects on physical activity. At the same time, the inclusion of a global for linear term retains the advantage of interpretability for other variables, particularly categorical covariates such as ethnicity and sex. The results obtained in our analysis are helpful from a public health perspective and may lead to new strategies for optimizing physical activity interventions in specific American subpopulations.

## 1 Introduction

Medical science is living in a golden age with the expansion of the clinical paradigms of digital and precision medicine [47, 25, 19]. In this new context, it is increasingly common to record patient information that is most faithfully represented by using complex statistical objects such as probability distributions [14, 13, 32, 33] that contain enriched information compared

---

\*ghosal@pstat.ucsb.edu

†marcos.matabuena@usc.es

‡AG and MM joint first co-authorship.

§meiring@pstat.ucsb.edu

¶petersen@stat.byu.edu

to traditional clinical biomarkers in predictive terms. Distributional representations can be seen as natural digital functional biomarkers to analyze wearable data information. In a series of papers, the performance of the distributional representation was compared with that of existing summary metrics, providing strong evidence of their advantages in diabetes and physical activity domains [13, 32, 33, 31]. Distributional representations are a direct functional extension of traditional compositional metrics [3, 1] and allow the creation of synthetic profiles over a continuum of intensities measured by wearable devices that provide an individualized profile of the patient’s activity. Importantly, these representations overcome the critical limitations of compositional metrics to define specific cut-off points to categorize patient information that can introduce subjectivity and be highly dependent on the population being analyzed.

This work is motivated by the desire to uncover factors that characterize the physical activity patterns of the American population recorded with the new distributional representation. As energetic expenditure behaves nonlinearly with age [45], and other anthropometrical measures [34], more advanced and flexible regression models are required to overcome the limitations of the linear model. Here, in order to provide a good balance between the advantages and disadvantages of linear models and non-linear models, we build on the partially linear model for scalar responses [26] and propose the first Partially Linear Fréchet Single Index model. As in the scalar response case, this can be viewed as an extension of the recently proposed global Fréchet regression and Fréchet single index models [40, 2, 12]. We incorporate the survey weights from the complex survey design of the NHANES into the model estimation to obtain reliable population-based results according to the composition of the US population [29].

From a public health point of view, the proposed model is attractive because it elucidates the impact certain variables exert on the American population’s physical activity levels in all ranges of accelerometer intensities. Moreover, these new findings can help to refine and plan specific health interventions that reduce the gap in physical inactivity in different US sub-populations. For example, one of the follow-up analyses conducted herein extracts clinical phenotypes of individuals to characterize the patients who are more or less active than predicted by the regression model.

The structure of the paper is as follows. Section 2 introduces the NHANES data that will be analyzed, together with a background of the physical activity distributional representations. Section 3 introduces the model and an efficient, spline-based estimator. Section 4 reports the various analyses performed. Finally, Section 5 discusses the results from a public health perspective, this paper’s role in the broader statistical literature on regression models in metric spaces, and its opportunities in the medical field to analyze other complex statistical objects.

## 1.1 Contributions

We briefly summarize the methodological contributions of this paper as well as the findings from analysis of the physical activity NHANES in regression models whose responses are the distributional physical activity representation.

- To our knowledge, we propose the first Partially Linear Fréchet Single Index regression model for responses that are probability distributions, viewed as elements of the Wasserstein metric space. Moreover, for this particular situation, we propose the use of splines for the first time in the Fréchet regression modeling framework.
- We propose an efficient modified optimization strategy to address the complex survey sampling mechanism of the NHANES data that retains the estimator’s form of a weighted least squares problem. The key idea of our approach is to estimate the model’s non-linear

component by means of regression splines after projecting the variables in this term to a single covariate.

- The primary findings of the NHANES analysis are:
  1. The proposed single-index model is shown to outperform the global Fréchet model in terms of  $R$ -square.
  2. Interpretations are provided for the effects of ethnicity and other interesting variables on distributional physical activity profiles. These novel analyses can provide new insights into how inactivity varies among sub-populations of the US country.
  3. We construct new physical activity phenotypes corresponding to individuals who do more or less exercise than is predicted by the model using the distributional representation. These analyses are new and help us examine how well individuals adhere to the recommended physical activity guidelines.

## 1.2 Literature review

Statistical regression analysis of response data in metrics spaces is a novel research direction in the statistical community [9, 4, 37, 49, 12, 39, 59, 7, 27, 20]. The first papers on hypothesis testing [6, 37], variable selection [50], semi-parametric regression models [12, 2], and non-parametric regression [15], have recently appeared. For classical regression models with univariate response data, the partially linear Single Index model has been a topic with particular popularity in the last twenty years in the statistical and econometrics literature [55]. There are several works in this direction, including recent extensions of the model to functional data [55, 53, 56, 60]. However, the authors are not aware of any existing extension to response data in metric spaces, even for the special case of distributional response data, or that incorporate the complex survey design into the analysis.

## 2 Motivation example: NHANES accelerometer data 2011-2014

We used data from the NHANES cohorts 2011 - 2014 [22]. The NHANES aims to provide a broad range of descriptive health and nutrition statistics for the non-institutionalized civilian U.S. population [22]. Data collection consists of an interview and an examination; the interview gathers personal demographic, health, and nutrition information; the examination includes physical measurements such as blood pressure, a dental examination, and the collection of blood and urine specimens for laboratory testing. Additionally, participants were asked to wear a physical activity monitor, starting on the day of their exam, and to keep wearing this device all day and night for seven full days (midnight to midnight) and remove it on the morning of the 9th day. The device used was the ActiGraph GT3X+ (ActiGraph of Pensacola, FL).

Physical activity signals were pre-processed by staff from the National Center for Health Statistics (NCHS) to determine signal patterns that were unlikely to be a result of human movement. Then, acceleration measurements were summarized at the minute level using Monitor-Independent Summary (MIMS) units, an open-source, device-independent universal summary metric [21]. In order to further increase the reliability of the analysis, we use the following filter criteria strategy extracted from [46] in order to remove participants with poor quality in their accelerometry data. Those participants who i) had fewer than three days of data with at least 10 hours of estimated wear time or were deemed by NHANES to have poor quality data ii) had non-wear periods, identified as intervals with at least 60 consecutive minutes of zero activity counts and at most 2 minutes with counts between 0 and 5 were

removed. These protocol instructions were adapted from high-level accelerometer research (see, for example, [48]).

## 2.1 Quantile distributional physical activity representations

We adopt a novel representation of the resulting data that extends previous compositional metrics to a functional setting [32], aimed at overcoming their dependency on certain physical activity intensity thresholds. This approach also overcomes some previously known limitations of more traditional approaches. Let  $i \in \{1, 2, \dots, n\}$  be the index for participants, where  $n$  is the total number of participants in the study. For the  $i$ -th participant, let  $M_i$  indicate the number of days (including partial days) for which accelerometer records are available and  $n_i$  be the number of observations recorded in the form of pairs  $(m_{ij}, A_{ij})$ ,  $j = 1, \dots, n_i$ . Here, the  $m_{ij}$  are a sequence of time points in the interval  $[0, M_i]$  in which the accelerometer records activity information, and  $A_{ij}$  is the measurement of the accelerometer at time  $m_{ij}$ .

In this paper, each individual’s accelerometer measurements  $\{A_{ij}\}_{j=1}^{n_i}$ ,  $i = 1, \dots, n$ , are studied without regard for their ordering. We consider the empirical quantile function,  $Y_i(t) = \hat{Q}_i(t)$ , for  $t \in [0, 1]$ , as the response in the regression model. Here,  $\hat{Q}_i = \hat{F}_i^{-1}$  is the generalized inverse of the empirical cumulative distribution function  $\hat{F}_i(a) = \frac{1}{n_i} \sum_{j=1}^{n_i} 1\{A_{ij} \leq a\}$ ,  $a \in \mathcal{R}$  for the physical activity values for the  $i$ -th individual. In order to illustrate clearly the difficulty of analyzing raw physical activity data in which different participants are monitored during different periods and in different experimental conditions, Figure 1 shows the plot of observed  $A_{ij}$  against  $m_{ij}$  for an arbitrary participant in our study (top panel). The bottom panel shows the empirical quantile functions of all participants after transforming the raw time series physical activity data into distributional quantile physical activity representation. Quantile physical activity representation overcomes the problem of summary physical activity when the raw time series have different lengths. In addition, the new representation uses all accelerometer intensities (over a continuum) to construct the new physical activity functional profile, unlike traditional representations of physical activity that summarize the information in the form of a compositional vector.

## 2.2 Details of covariates

A total of 4616 individuals were chosen for our analyses with physical activity monitoring available for at least 10 hours per day for four days. The covariates used in the model include sociodemographic, physical activity, dietary, and clinical variables such as age, Body Mass Index (BMI), Healthy Eating Index (HEI), Total Activity Count (TAC), along with the categorical variables Ethnicity and Sex. Age at the time of the analysis was in the range 20 to 80 years. The BMI ( $\text{Kg}/\text{m}^2$ ) was restricted to the range 18.5 – 40 to study individuals ranging from healthy to highly overweight/obese. The variable (HEI) was utilized indicating a Global score about the diet quality. TAC was the average over all activity counts over all the times activity was recorded for the device, in the notation of section 2.1, it is  $\sum_{j=1}^{n_i} A_{ij}/n_i$  for each  $i$ . The ethnicity variable reported racial origin of the participants divided in the following categories: Mexican American, Other Hispanic, Non-Hispanic White, Non-Hispanic Black, Non-Hispanic Asian, Other races including Multi-racial. To understand the distribution of the covariates between the levels of the Sex variable we constructed the Table 1.

This paper aims to create a parsimonious and straightforward regression model to interpret the several central aspects of energetic expenditure captured by the Age and BMI variables that are expected to behave in a non-linear way with the response. At the same time, we are interested in assessing the diet’s effect on physical exercise. We have observed that sex and ethnicity differences in the U.S population tend to interact in relation to physical activity,

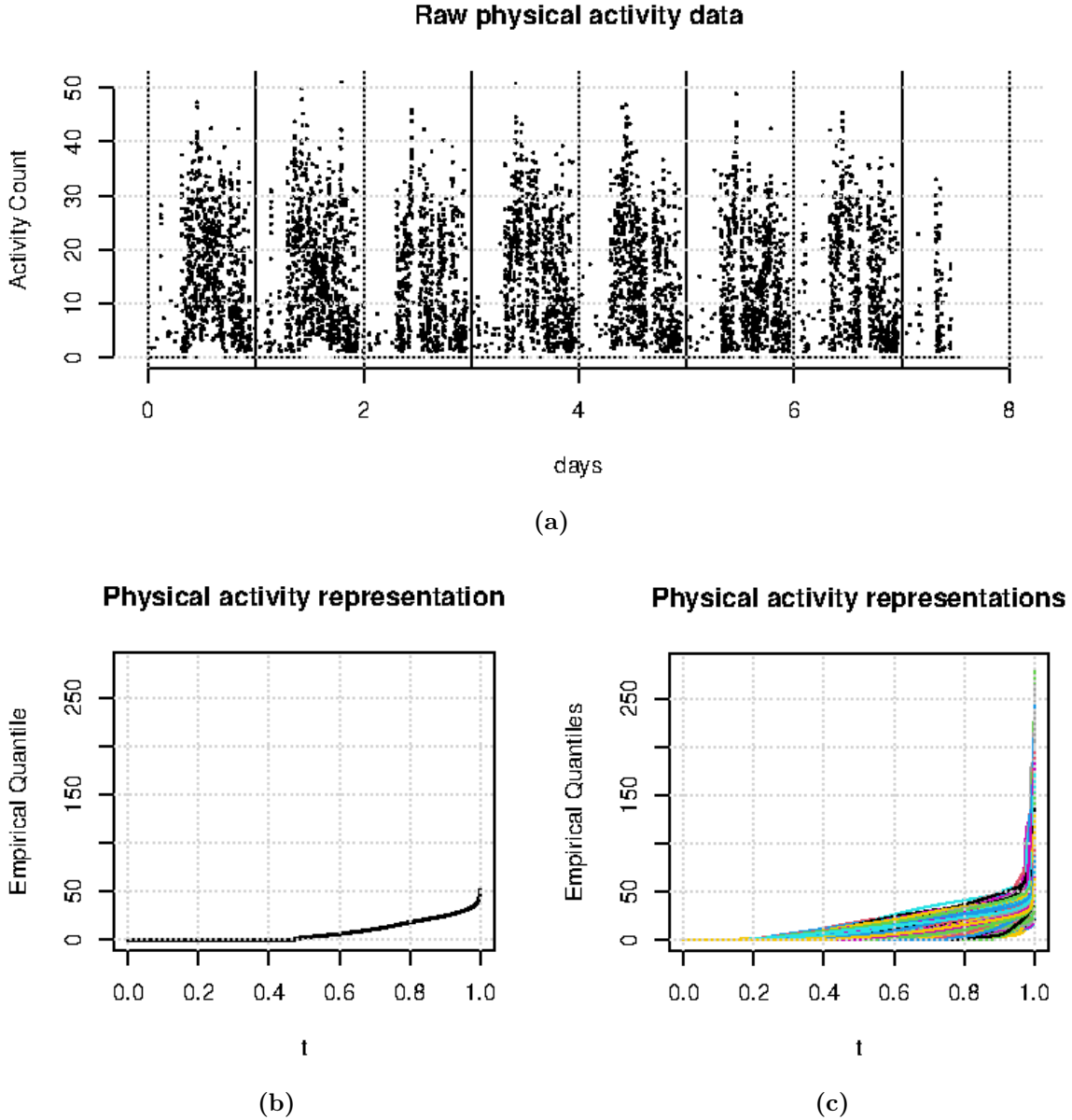


**Figure 1.** (a) The plot of physical activity time series  $A_{ij}$  of one representative participant (one chosen  $i$ ) in the NHANES 2011-2014 study monitored during 8 days are plotted over the observed time intervals  $m_{ij}$ , when the physical activity measurements are counted as described in the section 2.1. (b) The empirical quantile representation  $\hat{Q}_i$ , of the activity profile of the participant (chosen  $i$ ) described in (a) above, also described in the section 2.1. (c) The estimated empirical quantiles of physical activity profiles are computed from the empirical distribution from the raw time series for all 4616 participants in the study are plotted here. This helps to understand the quantile representation of the participant  $i$  in comparison with the rest of the participants in our study.

e.g., Black, White and Asian women tend to be physically more active than men while among the Mexican American and Other Hispanic ethnicities, men tend to be more active. Hence, we considered an interaction between sex and ethnicity to obtain reliable population-based conclusions about the relationships between these predictors and physical activity. The sample design of NHANES provides important advantages to obtain reliable population measurements that we cannot guarantee due to selection bias with observational cohorts such as the UK-biobank. In order to properly exploit this advantage, however, we must incorporate survey

**Table 1.** Summaries of the predictor variables Age, BMI (Body Mass Index), HEI (Healthy Eating Index), TAC (Total Activity Count), and Ethnicity used in the regression analysis, separated by the Sex. In the first column we distinguish the levels of the categorical variable ethnicity from the numerical covariates Age, BMI, HEI, TAC which are designated in the second column. In the third and fourth columns, the first four rows present the means and, in brackets, the standard deviations of the continuous variables (Age, BMI, HEI, and TAC) for Men and Women respectively. The rows 5 - 10 in the same columns represent the percentage breakdown of the sub-populations of Men and Women into their respective ethnicities. The description of the covariates are found in Section 2.2.

	Covariates	Men	Women
Numeric Variables	Age	47.45 (16.45)	48.082 (16.50)
	Body Mass Index	28.72 (5.73)	29.18 (7.41)
	Healthy Eating Index	53.013 (14.13)	56.63 (14.75)
	Total Activity Count	14342023 (3985616)	1382990 (3971762)
Ethnicities	Mexican American	8.55 %	6.42 %
	Other Hispanic	5.42 %	5.28 %
	Non-Hispanic White	70.65 %	72.3 %
	Non-Hispanic Black	8.82 %	10.29 %
	Non-Hispanic Asian	3.77 %	3.37 %
	Other Races Including Multi-racial	2.79 %	2.35 %

design in the estimation procedure, as described in Section 3.1 below.

### 3 The Partially Linear Fréchet Single-Index Regression model

Let  $Y_i$  be the quantile function of daily activity levels corresponding to the  $i$ -th participant. In what follows, we will build the regression by directly modeling the pointwise mean function of  $Y_i(t)$  on the covariates,  $t \in [0, 1]$ . The choice to use the quantile function as a characterization of the physical activity distribution can be explained as follows. First, because the distributions represented by the  $Y_i$  are a mixture of a mass at 0 and an absolutely continuous distribution for positive values, a density representation that ignores inactivity time is not appropriate. Moreover, the quantile function is practically less restrictive than, for example, the cumulative distribution function, which must take values between 0 and 1. Finally, and perhaps most importantly, the quantile function is known to be intimately connected to the well-established Wasserstein geometry on the space of distributions [52, 41, 36]. Briefly, if  $\mu$  and  $\nu$  are two suitable measures on  $\mathcal{R}$  with finite second moment, and if  $Q_\mu$  and  $Q_\nu$  are their corresponding quantile functions, then  $d_{W_2}(\mu, \nu)$ , the Wasserstein distance between  $\mu$  and  $\nu$ , is known to be equivalent to the  $L^2$  distance between  $Q_\mu$  and  $Q_\nu$ , that is,

$$d_{W_2}(\mu, \nu) = \left[ \int_0^1 (Q_\mu(t) - Q_\nu(t))^2 dt \right]^{1/2}. \quad (1)$$

As a consequence, under this metric, the Fréchet mean [11] measure of a random measure is characterized by the pointwise mean of the corresponding random quantile process. Hence, by proposing a regression model for the random quantile function  $Y_i$ , we are implicitly constructing a model for the conditional (Wasserstein-)Fréchet mean of the underlying random physical activity distribution measure [37].

Let  $\mathbf{X}_i \in \mathcal{R}^p$  denote the  $p$ -dimensional covariate vector that will appear in the single index part of the model, while  $\mathbf{Z}_i \in \mathcal{R}^q$  is the covariate vector considered for the linear part. The Partially Linear Fréchet Single Index model is

$$E(Y_i(t)|\mathbf{X}_i, \mathbf{Z}_i) = \alpha(t) + \beta(t)^T \mathbf{Z}_i + g(\boldsymbol{\theta}_0^T \mathbf{X}_i, t), \quad t \in [0, 1], \quad (2)$$



where the vector  $\boldsymbol{\theta}_0 \in \mathcal{R}^p$ , intercept function  $\alpha(t)$ , coefficient function  $\boldsymbol{\beta}(t)$  and link function  $g$  are the unknown parameters.

### 3.1 Model Estimation

For estimating the parameter  $\boldsymbol{\theta}_0$ , define parameter space

$$\Theta_p = \{\boldsymbol{\theta} \in \mathcal{R}^p : \|\boldsymbol{\theta}\|_E = 1, \text{ first non-zero element being strictly positive}\}$$

where  $\|\cdot\|_E$  is the Euclidean norm. To facilitate estimation of the smooth bivariate function  $g$ , we will use the expansion

$$g(u, t) \approx \sum_{k=1}^{K+s} \gamma_k(t) \phi_k(u), \quad (3)$$

where  $\{\phi_k\}_{k=1}^{K+s}$  is a B-spline basis of order  $s$  on a knot sequence of length  $K$ , and  $\gamma_k(t)$  are the coefficients of the basis as a function of  $t$ . With this approximation, the approximation to (2) that will motivate our estimator is

$$E(Y_i(t) | \mathbf{X}_i, \mathbf{Z}_i) \approx \alpha(t) + \boldsymbol{\beta}(t)^T \mathbf{Z}_i + \boldsymbol{\gamma}(t)^T \mathbf{U}_i(\boldsymbol{\theta}_0), \quad t \in [0, 1], \quad (4)$$

where  $\boldsymbol{\gamma}(t) = (\gamma_1(t), \dots, \gamma_{K+s}(t))^T$  and, for any  $\boldsymbol{\theta} \in \Theta_p$ ,  $\mathbf{U}_i(\boldsymbol{\theta}) = (\phi_1(\boldsymbol{\theta}^T \mathbf{X}_i), \dots, \phi_{K+s}(\boldsymbol{\theta}^T \mathbf{X}_i))^T$ .

The linear form of (4) suggests a semi-parametric least-squares approach for estimation. However, one must remember that the individuals we analyze from the NHANES database do not represent a simple random sample of the US population. Instead, they are the result of a structured sample of a complex survey design from a finite population of individuals. Therefore, in order to perform inference correctly and obtain reliable results according to the specific sample design of the NHANES dataset [29], it is necessary to adapt the usual estimation approach.

Assume that a sample  $\mathcal{D} = \{(Y_i, \mathbf{X}_i, \mathbf{Z}_i) : i \in S\}$  is available, where  $Y_i$  is a response variable, and  $\mathbf{X}_i, \mathbf{Z}_i$  are vectors of covariates taking values in a finite-dimensional space. The index set  $S$  represents a sample of  $n$  units from a finite population. To account for this sampling, each individual  $i \in S$  will be associated with a positive weight  $w_i$ . In our analyses, these weights were taken to be the inverse of the probability  $\pi_i > 0$  of being selected into the sample, i.e.  $w_i = 1/\pi_i$  [24, 28]. In order to introduce the sampling mechanism into the estimation procedure, we consider the Horvitz-Thompson estimator [17, 42], which is based on weights  $w_i$  that are proportional to the probability  $\pi_i$  of selecting the  $i$ -th individual in the experimental design, i.e.,  $w_i = 1/\pi_i$ .

Here, we adopt the Horvitz-Thompson approach in the estimation procedure through a weighted least squares criterion. The full procedure can be broken down into two steps. In the first step, for any unit-norm vector  $\boldsymbol{\theta}$  and any  $t \in [0, 1]$ , we can readily compute

$$\left( \hat{\alpha}_{\boldsymbol{\theta}}(t), \hat{\boldsymbol{\beta}}_{\boldsymbol{\theta}}(t), \hat{\boldsymbol{\gamma}}_{\boldsymbol{\theta}}(t) \right) = \underset{a \in \mathcal{R}, \mathbf{b} \in \mathcal{R}^q, \mathbf{c} \in \mathcal{R}^{K+s}}{\operatorname{argmin}} \sum_{i=1}^n w_i [Y_i(t) - a - \mathbf{b}^T \mathbf{z}_i - \mathbf{c}^T \mathbf{U}_i(\boldsymbol{\theta})]^2. \quad (5)$$

These estimates lead to initial fitted quantile functions

$$Y_i^*(\boldsymbol{\theta}, t) = \hat{\alpha}_{\boldsymbol{\theta}}(t) + \hat{\boldsymbol{\beta}}_{\boldsymbol{\theta}}^T(t) \mathbf{Z}_i + \hat{\boldsymbol{\gamma}}_{\boldsymbol{\theta}}^T(t) \mathbf{U}_i(\boldsymbol{\theta}), \quad t \in [0, 1]. \quad (6)$$

However, as a function of  $t$ , it may happen that  $Y_i^*(\boldsymbol{\theta}, t)$  is not monotonically increasing, and hence is not a valid quantile function. The typical solution for this is to project, in the  $L^2[0, 1]$  sense, this fitted value onto the nearest monotonic function [40, 37], yielding valid fitted quantile functions  $\hat{Y}_i(\boldsymbol{\theta}, t)$ .

Once these initial quantities are formed for any  $\boldsymbol{\theta}$  and  $t$ , we can proceed to the estimation of  $\boldsymbol{\theta}_0$ . As justified in [12], one can use a generalized version of the residual sums of squares to obtain the estimate. In the current context, we propose the survey-weighted criterion

$$W_n(\boldsymbol{\theta}) = \sum_{i=1}^n w_i \int_0^1 \left\{ Y_i(t) - \hat{Y}_i(\boldsymbol{\theta}, t) \right\}^2 dt \quad (7)$$

that constitutes a weighted average of the squared  $L^2$  norms of the quantile residuals (or, equivalently, of the squared Wasserstein distances between observed and fitted physical activity distributions). Then the estimated parameter is

$$\hat{\boldsymbol{\theta}} = \underset{\boldsymbol{\theta} \in \Theta_p}{\operatorname{argmin}} W_n(\boldsymbol{\theta}). \quad (8)$$

From this estimate of the index parameter, given any covariate pair  $(\mathbf{z}, \mathbf{x})$ , we can estimate the conditional Wasserstein-Fréchet mean quantile function as follows. First, the basis functions are evaluated at the relevant input by computing  $\hat{\mathbf{u}} = (\phi_1(\hat{\boldsymbol{\theta}}^T \mathbf{x}), \dots, \phi_{K+s}(\hat{\boldsymbol{\theta}}^T \mathbf{x}))^T$ . Then, as in (6), we construct the preliminary estimate

$$Y^*(t; \mathbf{z}, \mathbf{x}) = \hat{\alpha}_{\hat{\boldsymbol{\theta}}}(t) + \hat{\boldsymbol{\beta}}_{\hat{\boldsymbol{\theta}}}^T(t) \mathbf{z} + \hat{\boldsymbol{\gamma}}_{\hat{\boldsymbol{\theta}}}^T(t) \hat{\mathbf{u}}. \quad (9)$$

Finally, the estimated quantile function  $\hat{Y}(t; \mathbf{z}, \mathbf{x})$  is obtained by projecting, in the  $L^2$  sense,  $Y^*(t; \mathbf{z}, \mathbf{x})$  onto the space of quantile functions, meaning the nearest monotonically increasing function. In particular, for any set of observed covariates  $(\mathbf{Z}_i, \mathbf{X}_i)$ , we obtain fitted values  $\hat{Y}_i(t) = \hat{Y}(t; \mathbf{Z}_i, \mathbf{X}_i)$ .

### 3.2 Computational Details

We now provide details regarding our implementation of our estimator for the NHANES data base. In the models implemented below in Section 4, the non-linear covariate  $\mathbf{X}_i$  for the  $i$ -th individual consists of their BMI and age, so the dimension for this component of the model is  $q = 2$ , i.e.,  $\boldsymbol{\theta}_0 \in \Theta_2$ . For the spline basis in (3), computations were internally performed using the `dbs` function in the package `splines2` [54]. In our experiments, we set  $s = 4$  and  $K = 5$ , so the number of spline regression parameters is  $K + s = 9$ . Then, for a given  $\boldsymbol{\theta}$ , we obtain, for each order of quantile  $t$ , we obtain the sequence  $\mathcal{S}(\boldsymbol{\theta}, t) = \{\boldsymbol{\gamma}(t)^T \mathbf{u}_i : i = 1, 2, \dots, n\}$ . After ordering the elements from smallest to the largest, the minimum and the maximum values are considered the boundary knots, while the values corresponding to the following percentiles are considered the interior knots respectively: 16.667%, 33.333%, 50%, 66.667%, 83.333%. The covariates in the linear component  $\mathbf{Z}_i$  consist of HEI (continuous) and indicator variables for sex and ethnicity, as well as the interaction between these. The total number of covariates in this component is thus  $p = 12$ .

The estimates of parameters in (5) can be efficiently computed as a weighted least squares problem for any fixed  $\boldsymbol{\theta}$  and  $t \in [0, 1]$ , but in practice this can only be done for a finite ordered grid of values  $t \in T_m = \{t_1, \dots, t_m\} \subset [0, 1]$ . These initial survey-weighted least squares computations were done using R package `survey` [28, 29, 30], that allows us to introduce splines into the regression model while simultaneously computing and incorporating the weights  $w_i$  that are necessitated by the complex NHANES design. For any given  $\boldsymbol{\theta}$  and grid point  $t$ , computation of (6) is straightforward. To execute the projection step, observe that monotonicity can only be achieved in the discrete sense in dependence on the chosen grid  $T_m$ . We refer to [37] for a simple description of this projection algorithm, which can be done using any basic quadratic program solver. Consequently, for a given  $\boldsymbol{\theta}$ , (7) is approximated by numerical integration. Finally, to perform the optimization in (8), we use the function `optim` in R with



the L-BFGS-B algorithm by repeatedly performing the above steps to evaluate  $W_n(\boldsymbol{\theta})$  for different values of  $\boldsymbol{\theta}$  across iterations. To deal with the possibility of local minima, four different starting values (taken to be equally spaced in their angular representation) in  $\Theta_2$  were used for this optimization step, yielding (potentially) four local minimizers. The final estimator was taken as the one among these yielding the smallest value of  $W_n$ .

To understand the interaction of sex and ethnicity in physical activity levels, we computed the model estimates of the intercept for the different cases and plotted them in figure 3. The critical point in the interval derivation is considered for each intercept and  $t \in [0, 1]$ .

## 4 Experimental Results

We compare the performance between the new Partially Linear Fréchet Single-Index model and the global Fréchet model [40] in order to examine the relevant differences and advantages. The covariates used in the global Fréchet model are same as those in the PL-FSI model, just that in the former, all covariates are considered parts of the linear component. To begin, we evaluate the capacity of the models to explain differences in physical activity distributions across individuals using the survey-weighted  $R^2$  metric

$$R_{\oplus}^2 = 1 - \frac{\sum_{i=1}^n w_i \int_0^1 (Y_i(t) - \hat{Y}_i(t))^2 dt}{\sum_{i=1}^n w_i \int_0^1 (Y_i(t) - \bar{Y}(t))^2 dt} \quad (10)$$

where  $w_i$  is the survey weight corresponding to  $i$ -th observation and  $\bar{Y}(t) = (\sum_{i=1}^n w_i)^{-1} \sum_{i=1}^n w_i Y_i(t)$  is the weighted sample Wasserstein-Fréchet mean of the observed physical activity distributions. To compare models with different numbers of predictors, we define the adjusted Fréchet  $R^2$  as

$$\bar{R}_{\oplus}^2 = R_{\oplus}^2 - (1 - R_{\oplus}^2) \frac{q}{n - q - 1} \quad (11)$$

where  $n$  is the number of observations and  $q$  is the number of unknown parameters in the model [40]. In order to provide a measure of uncertainty for the estimates of the functional parameter  $\boldsymbol{\beta}$  corresponding to the linear component of (4), we provide an ad hoc confidence interval, with the following justification. For each fixed  $j \in \{1, \dots, q\}$ ,  $\boldsymbol{\theta} \in \Theta_p$ , and  $t \in [0, 1]$ , if the order of splines of the non-linear component is fixed and assuming no bias, the asymptotic distribution of the estimator  $\hat{\boldsymbol{\beta}}_{\boldsymbol{\theta}}(t)$  has been shown to be Gaussian in similar settings [5, 37]. We can then use the standard outputs of the `survey` package, which adjusts for the survey weights, to construct pointwise confidence bands for the functional coefficients  $\boldsymbol{\beta}(t)$ . Importantly, standard re-sampling strategies like a naive bootstrap do not work here with the two-step-sampling design of the NHANES because the observational units are not exchangeable. We emphasize that these confidence intervals are merely to guide our qualitative assessment of uncertainty, although their asymptotic precision has not been theoretically guaranteed due to sources of variability, including the effects of spline parameters and the estimation of  $\boldsymbol{\theta}_0$ , for which this procedure does not account.

### 4.1 Regression results

We began by fitting the Partially Linear Fréchet Single Index regression model that includes sex, ethnicity, HEI, and the interaction of sex, ethnicity as the variables in the linear component. Age and BMI were variables utilized in the non-linear component. All numerical covariates were centered and standardized prior to analysis. The estimated parameter for our model is  $\hat{\boldsymbol{\theta}} = (0.2661, 0.9639)$  for the ordered variables BMI and Age, reflecting a greater

influence of age compared to BMI in the constructed index. For the linear part of the model, the estimates  $\hat{\alpha}_{\theta}(t), \hat{\beta}_{\theta}(t)$  from equation (5) are shown along with their 95% confidence bands in the Figure 3 as functions of  $t \in [0, 0.97]$ . We only consider in the results,  $t \in [0, 0.97]$ , due to the inherent noise of the quantile physical representations in the far right tail. The pointwise confidence bands suggest differences between the most active individuals of the American and the Mexican individuals (reference group), where a significant decrease in physical activity values is seen in all percentiles. Importantly, in some ethnicities as Non-Hispanic Asian, women are more active than men. Regarding the diet effect captured by the HEI variable, the results show that it has a small potential effect, but only in the largest quantiles of physical activity.

In terms of the adjusted  $\bar{R}_{\oplus}^2$  metric from equation (11), the Partially Linear Fréchet Single Index model attained a value of 0.146, an approximate increase of 24% relative to the value 0.118 attained by the global Fréchet model. Thus, while these results indicate that the predictive capacity of the models are likely moderate, the additional parameters introduced by the single index and spline representation lead to a gain in the variance explained.

The estimates and their variance-covariance matrices are obtained from the function `vcov.svyglm` in the `survey` package in R that takes into account the complex survey design into the pointwise estimation and dependence structure estimation. The pointwise 95% Confidence Intervals of the intercepts for different cases of sex and ethnicity, as well as the parameter corresponding to HEI are plotted for  $t \in [0, 0.97]$  in figure 3. Importantly, the findings from these plots are interesting. As we can see, the physical activities vary with respect to ethnicities and with respect to sex within the ethnicities in different ways. Finally, For reproducibility of the results obtained, the code with the methods proposal here are publicly available on GitHub [https://github.com/aghosal89/FSI\\_NHANES\\_Application](https://github.com/aghosal89/FSI_NHANES_Application).

## 4.2 Phenotypes of physical exercise performed

Following the model fitting, a clustering analysis was performed on the quantile residuals  $\hat{e}_i(t) = Y_i(t) - \hat{Y}_i(t)$  from the fitted partially linear single-index Fréchet regression model, excluding the TAC variable as a predictor. The goal of this analysis is to identify physical activity clinical phenotypes [31] after adjusting for the effects of the relevant clinical variables that are included as predictors. For this purpose, we consider the clustering algorithm proposed in [10] that uses the energy distance and is available in the R `energy` package utilizing the `k-group` function. To select the number of clusters, we used the well-established elbow rule. According to this criterion, we estimated the within cluster sum of squares using the Gini mean difference for a different number of clusters, and we plotted the results. The number of clusters was then selected where there was a change in slope from steep to shallow (an elbow); in this case,  $k = 3$ .

Figure 2 shows the functional residual profiles of each cluster. Cluster 1 is composed of individuals who are more active than the model predicts (quantile residuals are positive for nearly all percentiles), particularly in the highest range of activity, and are therefore expected to be more healthy. In cluster 2 are the individuals of the American population that are less active than the model predicted. Finally, cluster 3 is a heterogeneous group involving individuals whose physical activity patterns are near those predicted by the model. As this type of clustering is somewhat obvious (positive, negative, and near zero), we further investigate the clusters relative to some covariates that were not included as predictors, due to not having causal biological effects on physical activity distributions. However, these variables are still associated with the individuals' health in terms of metabolic profiles.

From a public health perspective, the most interesting clusters to describe are the first two. Upon further analysis, the bottom row of Figure 2 indicates that physical activity is related to the patient's health condition in terms of better and worse metabolic profiles. For

example, the distribution of glucose values and creatinine take values in healthier ranges in cluster 1 compared to the others, as we observe in the boxplots. In addition, in order to discriminate and interpret the differences between clusters, the cluster-specific distributions of TAC are also helpful; the individuals belonging to cluster 1 are the most physically active in contrast to cluster 2. From a practical point of view, in terms of total energetic expenditure, we have formal criteria to determine when individuals adhere to the physical recommendations adjusting for potential confounders, i.e., the covariates used in the model such as ethnicity, BMI, age, HEI, and sex, that can have a significant effect in the comparison of the physical exercise performed. The analysis of the residuals drawn by the regression model allows us to do a standardized and harmonized of the deviation of physical exercise performed and compare the individuals of different characteristics and then reclassify the individuals by then expected physical activity performed.

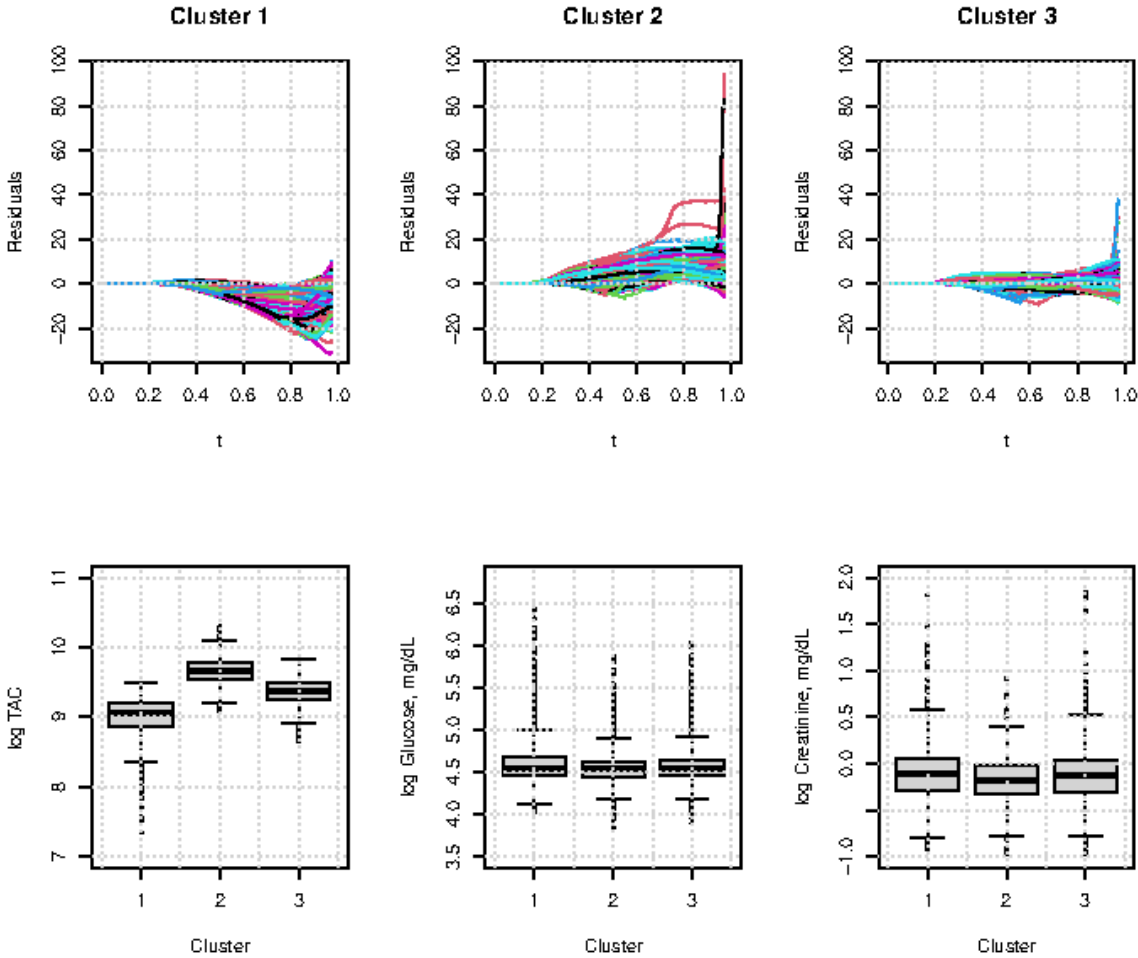


**Figure 2.** In the top row, the plots represent the raw functional residuals of the Partially Linear Fréchet Single Index model against the order of quantile  $t \in [0, 0.97]$ , belonging to the clusters 1, 2 and 3 respectively. The clusters are described in the Section 4.2. In the bottom row, the boxplots of distributions of the log of TAC variable, log of glucose (mg/ml), log of creatinine (mg/ml), across the clusters is shown.

### 4.3 Association with the non-linear covariates

Since BMI and age are considered in the ranges  $[18.5, 40]$  and  $[20, 80]$  respectively and they are in the non-linear component of the model, we were interested to interpret their effects

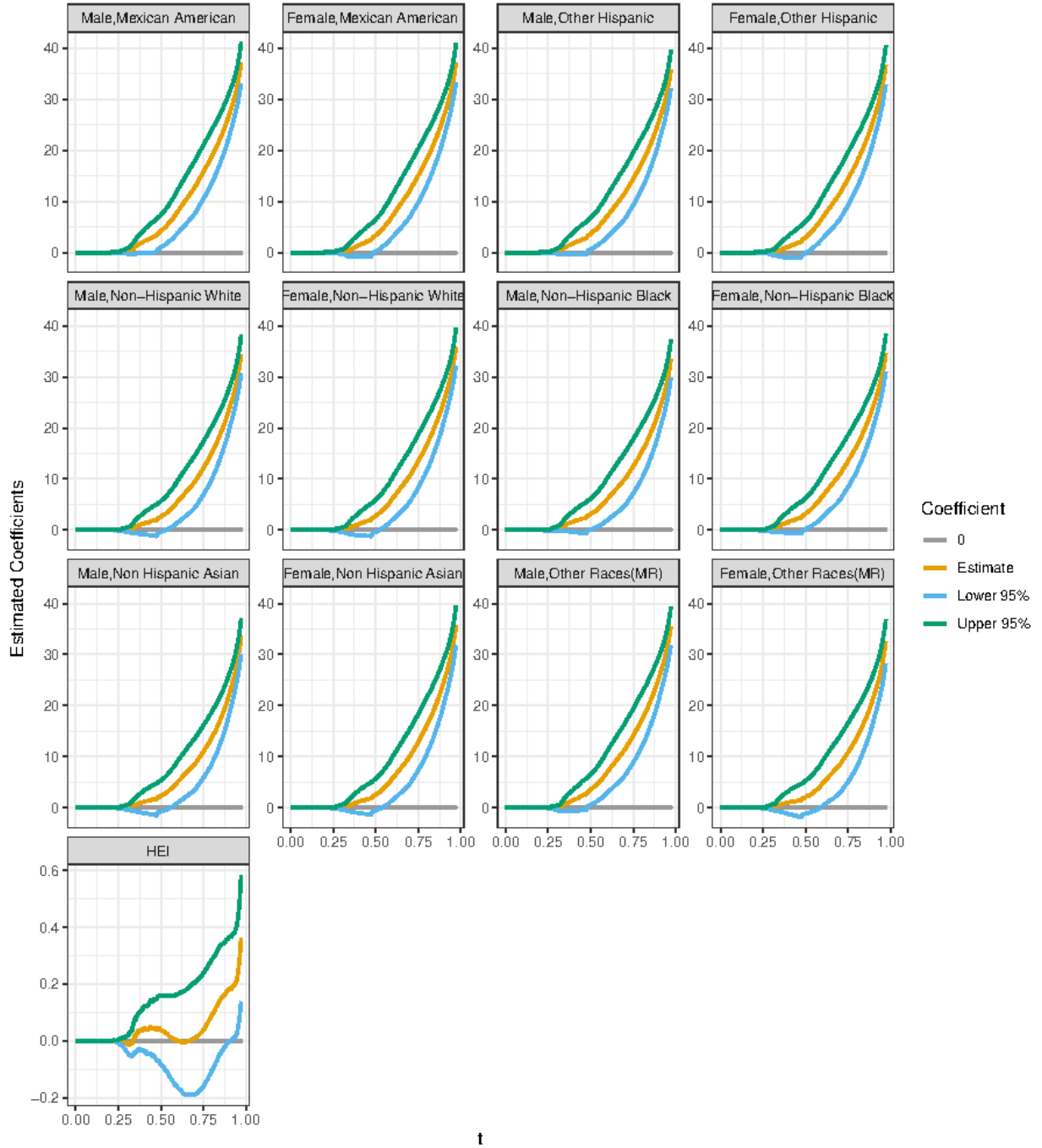


**Figure 3.** The estimates of the effects and their 95% Confidence Intervals obtained from the subsection 3.2 from the regression coefficients in the model (4) are shown here. The estimated effects are in orange color with a horizontal grey line at zero for reference. The green and blue curves represent the 95% pointwise upper and lower confidence bands, respectively as a function of  $t \in [0, 0.97]$ . We excluded the predicted quantiles for  $t > 0.97$  since near the boundary the estimates and their Confidence Intervals become unreliable. From the plot, the pointwise 95% Confidence Intervals of the regression parameters for the linear covariates do not include 0 for higher quantiles, implying significance at level 0.05.

on the mean of the physical activity quantile function, how these variables would affect the model prediction and performance. For the estimated index parameter  $\hat{\theta}$ , we obtained the single index  $\hat{\theta}^T \mathbf{X}$ , when  $\mathbf{X}$  is considered over a 2-dimensional grid. To predict the quantiles for each  $\mathbf{X}$  in the grid, the covariates in the linear component were fixed, as in, the

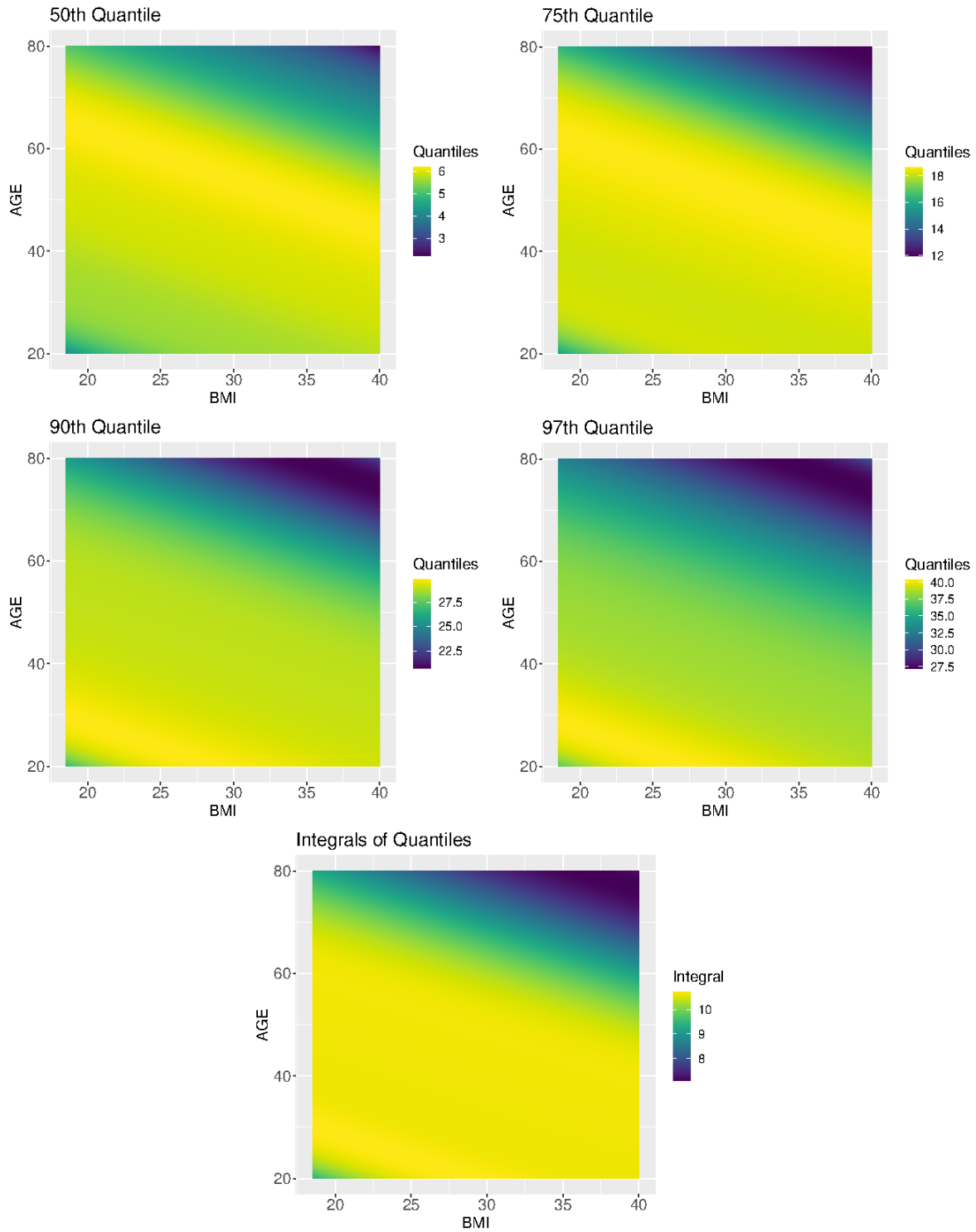


**Figure 4.** Heatmap plot of  $\hat{Y}(\hat{\theta}, t)$  across different quantiles,  $t = 0.50$  (top left),  $0.75$  (top right),  $0.90$  (second row left),  $0.97$  (second row right) respectively. The plot in the third row represents the integral  $\int_0^1 \hat{Y}(\hat{\theta}, t) dt$ . A 2-dimensional grid was considered for the covariates BMI (in range  $[18.5, 40]$ ) and age (in range  $[20, 80]$ ) for the single index component of the Partially Linear Fréchet Single-Index regression model. The categorical covariates in the linear component were fixed at their baseline levels (i.e. sex male, ethnicity Mexican American) while the numerical covariate HEI was fixed at median level. This plot describes the non-linear interaction in the conditional mean function between age and BMI.

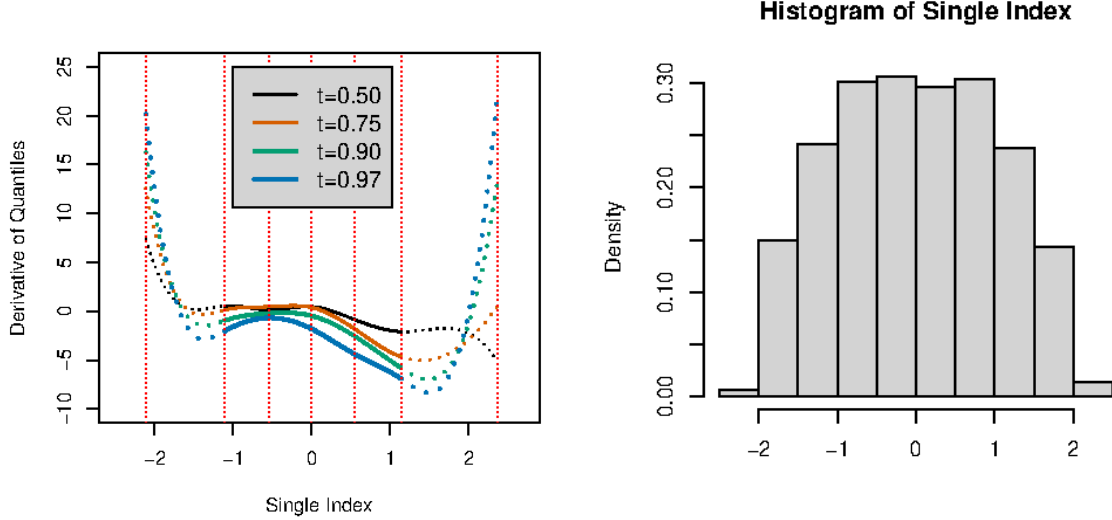


**Figure 5.** Left panel shows the plot of the derivative of the predicted quantiles with respect to the single index,  $\theta^T \mathbf{X}$  at the points on an equidistant grid of values constructed on the range of  $\theta^T \mathbf{X}_i$  for  $i = 1, 2, \dots, n$ . The selection process of knots was described in the section 3.2. The red dotted vertical lines represent these knots. This plot describes the non-linear interaction in the conditional mean function between age and BMI. Due to the boundary effects of the basis splines, the derivatives were not very reliable outside the penultimate knots. Hence, the derivatives between the 17.776-th and 83.333<sup>rd</sup> quantiles of the Single Index were shown with the solid line and outside the range were shown with dotted lines. The orders of the quantiles  $t = 0.50, 0.75, 0.90, 0.97$  being represented by colors black, red, green, and blue respectively with the thickness also increasing with  $t$  for better visual understanding. Right panel shows the histogram of the density of the Single Index value  $\hat{\theta}^T \mathbf{X}_i$  for  $i = 1, 2, \dots, n$ .

categorical covariates sex and ethnicity were fixed at their baseline level and the numeric covariate HEI was fixed at the median level. Hence, we computed the basis functions evaluated at  $\mathbf{X}$ ,  $\hat{\mathbf{u}} = (\phi_1(\hat{\theta}^T \mathbf{X}), \phi_2(\hat{\theta}^T \mathbf{X}), \dots, \phi_9(\hat{\theta}^T \mathbf{X}))$ . Hence,  $Y^*(t, \mathbf{z}, \mathbf{X})$  are obtained from equation (9) which then projected in  $L^2$  sense to the element in Wasserstein space,  $\hat{Y}(t, \mathbf{z}, \mathbf{X})$ . Figure 4 presents a heatmap for such predictions for selected values of the quantiles  $t = 0.50, 0.75, 0.90, 0.97$ . The BMI and age being in the horizontal and vertical axes respectively. We did plot for all quantiles on the grid, however, for  $t < 0.5$ , there was very little variation among the predicted quantiles and the predictions for  $t > 0.97$  were not interesting due to boundary effect of the basis splines.

The four plots at the top of Figure 4 indicate that the non-linear relationship between age and BMI is more substantial as the quantile increase, and this relationship is more robust in middle age and intermediate BMI values. As the value of the age increase and the BMI decrease, the individuals are more inactive, especially in the extremes.

For a better understanding of effect of the covariates on the model, we analyze the manner the prediction changes with respect to the projection  $\theta^T \mathbf{X}$ . For this purpose, we studied the analytic derivative of  $Y^*(t, \mathbf{z}, \mathbf{X}_l)$  with respect to the single index  $\hat{\theta}^T \mathbf{X}_l$  in the equation (12) below:

$$\frac{\partial}{\partial(\hat{\theta}^T \mathbf{x})} Y^*(t, \mathbf{z}, \mathbf{x}) = \left[ \sum_j \hat{\gamma}_j(t) \phi'_j(\hat{\theta}^T \mathbf{x}) \right] \quad (12)$$

The derivative of 1<sup>st</sup> order of the B-splines was computed in R using the function `dfs` in the



package `splines2`. This derivative was computed for each of the points  $\{\hat{\theta}^T \mathbf{X}_1, \hat{\theta}^T \mathbf{X}_2, \dots, \hat{\theta}^T \mathbf{X}_n\}$  using the equation (12) and for the quantiles  $t = 0.50, 0.75, 0.90, 0.97$ . The left panel of the figure 5 displays the plot, which indicates that the index involving BMI and age has little or no effect (ignoring the boundaries) until the index value gets above 1, approximately, after which it has a negative effect. This means that, given the other variables in the linear term, BMI and age only start to have an effect for large BMI/age combinations, and the effect gets stronger as this index increases. Also, the effect is stronger in the tail (larger values of  $t$ ) and not very strong for the median of the Quantile function.

#### 4.4 Variation in number of daily steps and non-linear covariates

A critical point in the interpretation of our results from a practical point of view is to examine the clinical significance of the one-unit variation of the Monitor Independent Movement Summary Unit (MIMS) in human health. To the best of our knowledge, no paper has addressed this issue. However, the following article [23] offers the equivalences between the various accelerometer units, e.g., MIMS and EMMO. Then, according to the following EMMO metric paper [44], which shows that a variation of 1 mg is 500 steps per day and changes in the annual mortality of 2 – 3 % and hazard ratio of 0.95; and extrapolate the overall change in steps and another clinical outcome. In particular, in our setting, 1 MIMS daily unit variations e.g  $\int_0^1 Q(t)dt$  is equivalent in inactive people to 1000 daily/steps and 4 percent in annual mortality.

The last graphic of Figure 4 shows the variation in the number of steps per day of the non-linear variables that is equivalent approximately to the integral of the quantile variable e.g  $\int_0^1 Q(t)dt$  (TAC variable). We show that only for the effect of the age in terms of conditional mean regression functions can be a variation of 2000 steps between young and elderly patients than corresponding changes in annual mortality around 8 percent. Regarding body mass, an increase of  $20kg/m^2$  percent in the BMI can induce causal variations of more than 1000 steps and consequently, increases the human mortality around 4 percent.

## 5 Discussion

The core contribution of this paper is to propose a new Partially Linear Fréchet Single Index regression model to analyze responses of distributional functional nature. Importantly, the new methods have been implemented to analyze the physical activity data from NHANES 2011-2014 that follow a complex survey design. We incorporate survey weights within the new Partially Linear Fréchet single index algorithm to handle the weighted squared loss function according to the sampling mechanism induced by the estimator Horvitz-Thompson [24].

The applications of the new methods in the NHANES dataset in individuals between 20-80 years old drive new findings in the physical activity literature that we summarized below:

1. We examine the discrepancies between different ethnicities in the American population’s physical activity levels across the sexes, and the continuous variable HEI, BMI, and age, in all ranges of human physical activity intensities thanks to the use of new physical activity quantile distributional representations. For example, we show that diet is only important in the physical activity levels in the high-intensity range; a more positive diet according to HEI score is related to more exercise. We also show that the Mexican group is the most active individuals in the American population, and we discover a non-linear interaction between age and BMI in the energetic expenditure, specifically in higher quantiles probabilities.

2. We characterize individuals that are more active and inactive than we expected according to the results drawn by the regression model in cluster analysis. These results can have significant implications from the public health perspective because they can help program-specific interventions to combat the inactivity in different subpopulations in U.S. populations.
3. We show the modeling advantages of the new Fréchet Single Index algorithm in predicting the distributional representations compared to the classical global Fréchet regression model in terms of adjusted Fréchet R-squared and in terms of interpretability with the new tools introduced, e.g., the gradient of a conditional mean function, in which we prove that the non-linearly effect is in middle age individuals with low BMI.

From a methodological point of view, we propose the first Partially Linear Fréchet Single Index regression model in the context of responses in metric spaces to overcome some limitations of the lack of flexibility of the global Fréchet model. At the same time, we preserve the interpretability advantages of linear regression along with a subset of predictors.

To the best of our knowledge, this is also the first regression model to incorporate survey data in the context of responses in metrics spaces and also the first work that we consider the estimation of the gradient of the conditional mean function in order to interpret the local contribution of each predictor in each order of the Quantile functional response [16].

The finite-dimensional compositional metrics are the most popular approach to analyzing accelerometer data. Here we consider using their functional extension [32] to capture more information about physical activity from an individual. By adopting the mathematical framework of statistical analysis in metric spaces with the  $L^2$ -Wassertein or another Wasserstein metric to handle the functional compositional representations, we overcome the problems of zero with compositional data. In addition, the range of values measured by the accelerometer varies widely between individuals and groups, which can present difficulties when trying to apply the standard distributional data analysis methods in our setting [32], for example, functional compositional transformations [51, 38, 18] that can be an alternative strategy to create a regression model about physical activity in a linear space using for such purpose the vast literature of unconstrained functional response regression models. From a methodological point of view, the distributional physical activity representation arises from a mixed-stochastic process (see Figure 1 for more details) that prevents to use the of linear functional data methods based on considering a basis of functions due to the discontinuity of the quantile function in the transition of the inactivity to activity in the physical exercise.

The analysis of complex statistical objects in biomedical science provides an excellent opportunity to create new clinical biomarkers that enrich the information more than existing variables that monitor the health and evolution of diseases. Distributional representations are a significant advancement in digital medicine [19] as a digital biomarker [58, 33]. However, the generality of techniques introduced, provides users the opportunity to use the methods developed here with other complex statistical objects such as connectivity graphs, shape, and directional objects that can introduce new clinical findings in a broad list of clinical situations for example in the brain and phylogenetic tree analysis [43, 59, 35, 8, 8, 57]. Furthermore, with the increasing analysis of large cohorts with richer designs such as complex survey design, the methods provided here will gain more popularity among practitioners, and the use of complex statistical objects will undoubtedly be a daily statistical practice in biomedical applications.

## References

- [1] Tadej Battelino, Thomas Danne, Richard M Bergenstal, Stephanie A Amiel, Roy Beck, Torben Biester, Emanuele Bosi, Bruce A Buckingham, William T Cefalu, Kelly L Close,

- et al. Clinical targets for continuous glucose monitoring data interpretation: recommendations from the international consensus on time in range. *Diabetes Care*, 42(8):1593–1603, 2019.
- [2] Satarupa Bhattacharjee and Hans-Georg Müller. Single index fréchet regression. *arXiv preprint arXiv:2108.05437*, 2021.
- [3] Lyvia Biagi, Arthur Bertachi, Marga Giménez, Ignacio Conget, Jorge Bondia, Josep Antoni Martín-Fernández, and Josep Vehí. Individual categorisation of glucose profiles using compositional data analysis. *Statistical Methods in Medical Research*, 28(12):3550–3567, 2019.
- [4] Yaqing Chen, Zhenhua Lin, and Hans-Georg Müller. Wasserstein regression. *Journal of the American Statistical Association*, pages 1–14, 2021.
- [5] Erjia Cui, Andrew Leroux, Ekaterina Smirnova, and Ciprian M. Crainiceanu. Fast univariate inference for longitudinal functional models. *Journal of Computational and Graphical Statistics*, 31(1):219–230, 2022.
- [6] Paromita Dubey and Hans-Georg Müller. Fréchet analysis of variance for random objects. *Biometrika*, 106(4):803–821, 2019.
- [7] Paromita Dubey and Hans-Georg Müller. Modeling time-varying random objects and dynamic networks. *Journal of the American Statistical Association*, pages 1–16, 2021.
- [8] Paromita Dubey and Hans-Georg Müller. Modeling time-varying random objects and dynamic networks. *Journal of the American Statistical Association*, 0(0):1–16, 2021.
- [9] Jianing Fan and Hans-Georg Müller. Conditional wasserstein barycenters and interpolation/extrapolation of distributions. *arXiv preprint arXiv:2107.09218*, 2021.
- [10] Guilherme Franca, Maria Rizzo, and Joshua T Vogelstein. Kernel k-groups via hartigan’s method. *IEEE Transactions on Pattern Analysis and Machine Intelligence*, 2020.
- [11] Maurice Fréchet. Les éléments aléatoires de nature quelconque dans un espace distancié. *Annales de l’Institut Henri Poincaré*, 10:215–310, 1948.
- [12] Aritra Ghosal, Wendy Meiring, and Alexander . Fréchet single index models for object response regression. *arXiv preprint arXiv:2108.06058*, 2021.
- [13] Rahul Ghosal, Vijay R Varma, Dmitri Volfson, Inbar Hillel, Jacek Urbanek, Jeffrey M Hausdorff, Amber Watts, and Vadim Zipunnikov. Distributional data analysis via quantile functions and its application to modeling digital biomarkers of gait in Alzheimer’s Disease. *Biostatistics*, 11 2021. kxab041.
- [14] Rahul Ghosal, Vijay R Varma, Dmitri Volfson, Jacek Urbanek, Jeffrey M Hausdorff, Amber Watts, and Vadim Zipunnikov. Scalar on time-by-distribution regression and its application for modelling associations between daily-living physical activity and cognitive functions in alzheimer’s disease. *Scientific Reports*, 12(1):1–16, 2022.
- [15] Steve Hanneke. Universally consistent online learning with arbitrarily dependent responses. In *International Conference on Algorithmic Learning Theory*, pages 488–497. PMLR, 2022.
- [16] Trevor Hastie and Clive Loader. Local regression: Automatic kernel carpentry. *Statistical Science*, pages 120–129, 1993.

- [17] Daniel G Horvitz and Donovan J Thompson. A generalization of sampling without replacement from a finite universe. *Journal of the American statistical Association*, 47(260):663–685, 1952.
- [18] Karel Hron, Alessandra Menafoglio, Matthias Templ, K Hruuzova, and Peter Filzmoser. Simplicial principal component analysis for density functions in bayes spaces. *Computational Statistics & Data Analysis*, 94:330–350, 2016.
- [19] Aamir Javaid, Fawzi Zghyer, Chang Kim, Erin M Spaulding, Nino Isakadze, Jie Ding, Daniel Kargillis, Yumin Gao, Faisal Rahman, Donald E Brown, et al. Medicine 2032: The future of cardiovascular disease prevention with machine learning and digital health technology. *American Journal of Preventive Cardiology*, page 100379, 2022.
- [20] Jeong Min Jeon, Young Kyung Lee, Enno Mammen, and Byeong U. Park. Locally polynomial Hilbertian additive regression. *Bernoulli*, 28(3):2034 – 2066, 2022.
- [21] Dinesh John, Qu Tang, Fahd Albinali, and Stephen Intille. An open-source monitor-independent movement summary for accelerometer data processing. *Journal for the Measurement of Physical Behaviour*, 2(4):268–281, 2019.
- [22] Clifford Leroy Johnson, Sylvia M Dohrmann, Vicki L Burt, and Leyla Kheradmand Mohadjer. *National health and nutrition examination survey: sample design, 2011–2014*. Number 2014. US Department of Health and Human Services, Centers for Disease Control and Prevention, National Center for Health Statistics, 2014.
- [23] Marta Karas, John Muschelli, Andrew Leroux, Jacek K Urbanek, Amal A Wani-gatunga, Jiawei Bai, Ciprian M Crainiceanu, Jennifer A Schrack, et al. Comparison of accelerometry-based measures of physical activity: Retrospective observational data analysis study. *JMIR mHealth and uHealth*, 10(7):e38077, 2022.
- [24] Leslie Kish. *Survey Sampling*. Number 04; HN29, K5. 1965.
- [25] Xiao Li, Jessilyn Dunn, Denis Salins, Gao Zhou, Wenyu Zhou, Sophia Miryam Schüssler-Fiorenza Rose, Dalia Perelman, Elizabeth Colbert, Ryan Runge, Shannon Rego, Ria Sonecha, Somalee Datta, Tracey McLaughlin, and Michael P. Snyder. Digital health: Tracking physiomes and activity using wearable biosensors reveals useful health-related information. *PLOS Biology*, 15(1):1–30, 01 2017.
- [26] Hua Liang, Xiang Liu, Runze Li, and Chih-Ling Tsai. Estimation and testing for partially linear single-index models. *Annals of Statistics*, 38(6):3811, 2010.
- [27] Zhenhua Lin, Hans-Georg Müller, and Byeong U Park. Additive models for symmetric positive-definite matrices, riemannian manifolds and lie groups. *arXiv preprint arXiv:2009.08789*, 2020.
- [28] Thomas Lumley. Analysis of complex survey samples. *Journal of Statistical Software*, 9:1–19, 2004.
- [29] Thomas Lumley. *Complex Surveys: A Guide to Analysis Using R*. John Wiley and Sons, 2010.
- [30] Thomas Lumley. survey: analysis of complex survey samples, 2020. R package version 4.0.

- [31] Marcos Matabuena, Paulo Félix, Ziad Akram Ali Hammouri, Jorge Mota, and Borja del Pozo Cruz. Physical activity phenotypes and mortality in older adults: a novel distributional data analysis of accelerometry in the nhanes. *Aging Clinical and Experimental Research*, Oct 2022.
- [32] Marcos Matabuena and Alexander Petersen. Distributional data analysis of accelerometer data from the nhanes database using nonparametric survey regression models. *arXiv preprint arXiv*, 2104, 2021.
- [33] Marcos Matabuena, Alexander Petersen, Juan C Vidal, and Francisco Gude. Glucodensities: a new representation of glucose profiles using distributional data analysis. *Statistical methods in medical research*, 2021.
- [34] Jigar N Mehta, Ashish V Gupta, Nidhi G Raval, Nishu Raval, and Nidhi Hasnani. Physiological cost index of different body mass index and age of an individual. *National Journal of Physiology, Pharmacy and Pharmacology*, 7(12):1313–1317, 2017.
- [35] Tom MW Nye, Xiaoxian Tang, Grady Weyenberg, and Ruriko Yoshida. Principal component analysis and the locus of the fréchet mean in the space of phylogenetic trees. *Biometrika*, 104(4):901–922, 2017.
- [36] Victor M Panaretos and Yoav Zemel. Statistical aspects of Wasserstein distances. *Annual Review of Statistics and its Application*, 6:405–431, 2019.
- [37] Alexander Petersen, Xi Liu, and Afshin A Divani. Wasserstein  $f$ -tests and confidence bands for the fréchet regression of density response curves. *The Annals of Statistics*, 49(1):590–611, 2021.
- [38] Alexander Petersen, Hans-Georg Müller, et al. Functional data analysis for density functions by transformation to a hilbert space. *The Annals of Statistics*, 44(1):183–218, 2016.
- [39] Alexander Petersen and Hans-Georg Müller. Functional data analysis for density functions by transformation to a hilbert space. *Ann. Statist.*, 44(1):183–218, 02 2016.
- [40] Alexander Petersen and Hans-Georg Müller. Fréchet regression for random objects with euclidean predictors. *Ann. Statist.*, 47(2):691–719, 04 2019.
- [41] Gabriel Peyré, Marco Cuturi, et al. Computational optimal transport: With applications to data science. *Foundations and Trends® in Machine Learning*, 11(5-6):355–607, 2019.
- [42] Sophia Rabe-Hesketh and Anders Skrondal. Multilevel modelling of complex survey data. *Journal of the Royal Statistical Society: Series A (Statistics in Society)*, 169(4):805–827, 2006.
- [43] Jesús D Arroyo Relión, Daniel Kessler, Elizaveta Levina, and Stephan F Taylor. Network classification with applications to brain connectomics. *The Annals of Applied Statistics*, 13(3):1648, 2019.
- [44] Alex Rowlands, Melanie Davies, Paddy Dempsey, Charlotte Edwardson, Cameron Razieh, and Thomas Yates. Wrist-worn accelerometers: recommending  $\sim 1.0$  mg as the minimum clinically important difference (mcid) in daily average acceleration for inactive adults. *British Journal of Sports Medicine*, 55(14):814–815, 2021.
- [45] Jennifer A. Schrack, Eleanor M. Simonsick, Paulo H.M. Chaves, and Luigi Ferrucci. The role of energetic cost in the age-related slowing of gait speed. *Journal of the American Geriatrics Society*, 60(10):1811–1816, 2012.

- [46] Ekaterina Smirnova, Andrew Leroux, Quy Cao, Lucia Tabacu, Vadim Zipunnikov, Ciprian Crainiceanu, and Jacek K Urbanek. The predictive performance of objective measures of physical activity derived from accelerometry data for 5-year all-cause mortality in older adults: National health and nutritional examination survey 2003–2006. *The Journals of Gerontology: Series A*, 2019.
- [47] Eric J. Topol. A decade of digital medicine innovation. *Science Translational Medicine*, 11(498), 2019.
- [48] Richard P Troiano, David Berrigan, Kevin W Dodd, Louise C Masse, Timothy Tillet, Margaret McDowell, et al. Physical activity in the United States measured by accelerometer. *Medicine and Science in Sports and Exercise*, 40(1):181, 2008.
- [49] Danielle C Tucker. *Modeling Non-Euclidean Data via Fréchet Regression*. PhD thesis, University of Illinois at Chicago, 2022.
- [50] Danielle C Tucker, Yichao Wu, and Hans-Georg Müller. Variable selection for global fréchet regression. *Journal of the American Statistical Association*, pages 1–15, 2021.
- [51] Karl Gerald Van den Boogaart, Juan José Egozcue, and Vera Pawlowsky-Glahn. Bayes hilbert spaces. *Australian & New Zealand Journal of Statistics*, 56(2):171–194, 2014.
- [52] Cédric Villani. *Optimal transport: old and new*, volume 338. Springer, 2009.
- [53] Jane-Ling Wang, Jeng-Min Chiou, and Hans-Georg Müller. Functional data analysis. *Annual Review of Statistics and Its Application*, 3:257–295, 2016.
- [54] Wenjie Wang and Jun Yan. Shape-restricted regression splines with r package splines2. *Journal of Data Science*, 19(3):498–517, 2021.
- [55] Raymond K. W. Wong, Yehua Li, and Zhengyuan Zhu. Partially linear functional additive models for multivariate functional data. *Journal of the American Statistical Association*, 114(525):406–418, 2019.
- [56] Weiwei Xiao, Yixuan Wang, and Haiyan Liu. Generalized partially functional linear model. *Scientific reports*, 11(1):1–14, 2021.
- [57] Ying Yuan, Hongtu Zhu, Weili Lin, and James Stephen Marron. Local polynomial regression for symmetric positive definite matrices. *Journal of the Royal Statistical Society: Series B (Statistical Methodology)*, 74(4):697–719, 2012.
- [58] Jingru Zhang, Kathleen R Merikangas, Hongzhe Li, and Haochang Shou. Two-sample tests for multivariate repeated measurements of histogram objects with applications to wearable device data. *The Annals of Applied Statistics*, 16(4):2396–2416, 2022.
- [59] Yidong Zhou and Hans-Georg Müller. Dynamic network regression. *arXiv preprint arXiv:2109.02981*, 2021.
- [60] Hanbing Zhu, Riquan Zhang, Yanghui Liu, and Hui Ding. Robust estimation for a general functional single index model via quantile regression. *Journal of the Korean Statistical Society*, pages 1–30, 2022.